

A novel fluorescent turn-on probe for bisulfite based on NBD chromophore

PUHUI XIE*[§], GUANGQIN GAO[§], WENJIE ZHANG, GUOYU YANG and QIU JIN
College of Sciences, Henan Agricultural University, Zhengzhou 450002, P. R. China
e-mail: phxie2013@163.com

MS received 31 December 2014; revised 2 April 2015; accepted 4 April 2015

Abstract. A novel fluorescent turn-on probe (compound **1**) for bisulfite based on 7-nitrobenz-2-oxa-1,3-diazole (NBD) chromophore has been developed. Its sensing behavior toward various anions was investigated by absorption and fluorescence techniques. This probe shows a selective, turn-on fluorescent response and ratiometric colorimetric response toward bisulfite in aqueous acetonitrile solutions. The possible recognition mechanism of probe **1** toward bisulfite was illustrated by MS spectra analysis and DFT calculations. Probe **1** was used to determine bisulfite in real-life samples with good recoveries.

Keywords. Fluorescent probe; turn-on; NBD chromophore; bisulfite.

1. Introduction

Fluorescence spectroscopy has become a powerful technique for sensing and imaging trace amounts of fluorescent samples due to its simplicity, sensitivity, fast response times, as well as its application for *in vivo* imaging. The exploration of fluorescent probes for anions has attracted considerable attention in recent years because many biological processes involve molecular recognition of anionic species.^{1–5}

However, due to their diverse geometries, charge distributions, sizes and high enthalpies of hydration of anions, which present an obvious obstacle to develop probes with abilities to function in aqueous media, it is very difficult to develop anion recognition systems.⁶ Even so, various probes for anions have been developed based on noncovalent interactions such as hydrogen bonding,^{7–11} electrostatic interactions^{12–17} or displacement reaction through coordination with metal complexes.^{18–21} A special chemical reaction between a receptor and target species will give a unique spectroscopic change and provide us versatile means to investigate a wide range of analytes with superior selectivity.^{22,23} Hydrogen bonding is an important noncovalent force often involved in the formation of supramolecular structures. In the area of photophysics, it has been generally recognized that formation of hydrogen bonds can restrict the intramolecular rotations, and rigidify the molecular structures, and help to minimize the nonradiative energy losses of the excitons

and maximize the probability of radiative transition, resulting in turn-on of the emission.

Bisulfite is one of the anions that has been widely used as an additive in foods, beverages and pharmaceutical products. It acts as an antimicrobial agent, enzyme inhibitor and antioxidant.^{24–29} However, bisulfite in certain concentrations has been associated with allergic reaction and food intolerance symptoms, such as difficulty in breathing, wheezing, hives, and gastrointestinal distress.^{30–34} Therefore, development of a sensitive and selective fluorescent sensor for the determination of bisulfite is of great importance for food safety and quality control, clinical and environmental applications.

In this work, we introduced pyrrole group to 7-nitrobenz-2-oxa-1,3-diazole (NBD) fluorophore to construct a HSO_3^- -selective sensor. NBD was chosen as the fluorophore because of long emission wavelength, good cell permeability and applications in chemical biology and bioanalytical studies.^{35–37} The pyrrole-functionated NBD derivative (scheme 1) was expected to interact with HSO_3^- through hydrogen bonding, producing a strongly fluorescent HSO_3^- adduct of the receptor.

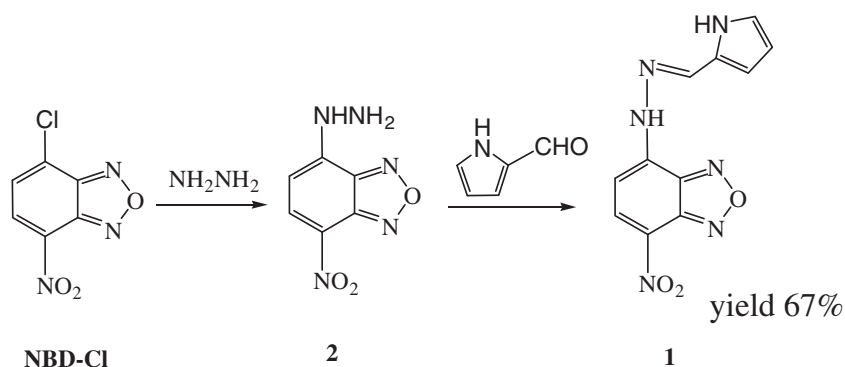
2. Experimental

2.1 Reagents and apparatus

Acetonitrile of spectroscopic grade and deionized water (or distilled) were used throughout the experiment as solvents. All the chemicals of analytical grade for syntheses were purchased from commercial suppliers and were used without further purification. NMR spectra

*For correspondence

[§] Puhui Xie and Guangqin Gao are contributed equally to this work.



Scheme 1. General procedure for the synthesis of probe **1**.

were recorded with a 400 MHz Varian spectrometer. Electrospray ionization mass spectra (ESI-MS) were measured on a micrOTOF-Q II system. Absorption spectra were obtained on a TU1901 Ultraviolet–visible spectrophotometer. The fluorescence spectra were measured with a Cary Eclipse fluorescence spectrometer.

2.2 Syntheses

Compound **2** was prepared similar to the reported procedures by using NBD-Cl and hydrazine hydrate as raw materials.³⁸ Hydrazine monohydrate (1.5 mL, 30 mmol) in 20 mL CH₃OH was added in dropwise to a solution of NBD-Cl (200 mg, 1 mmol) in 20 mL CHCl₃. The resulting solution was stirred at room temperature for 3 h. A yellowish-brown precipitate appeared gradually. It was filtered and washed with small amount of CHCl₃, then dried under vacuum at 50°C to get the desired product (140 mg, 84%), which was used for the next step without further purification.

2-Pyrrole aldehyde (234 mg, 2.5 mmol) was added to a solution of compound **2** (160 mg, 0.82 mmol) in 6 mL absolute ethanol. One drop of acetic acid was added to catalyze the reaction. The mixture was stirred at room temperature for 20 h. The solvent was evaporated *in vacuo*. The residue was purified by column chromatography on silica gel with ethyl acetate/hexanes (1/3, v/v) to afford a dark red solid of 0.13 g in 67% yield. ¹H NMR (DMSO-*d*₆, δ, ppm), 12.95 (s, 1H), 11.79 (s, 1H), 8.59 (d, *J* = 9.2 Hz, 1H), 8.43 (s, 1H), 7.18 (d, *J* = 9.2 Hz, 1H), 7.11 (d, *J* = 8.0 Hz, 1H), 6.66 (s, 1H), 6.22–6.24 (m, 1H) (figure S1 in Supplementary information). ¹³C NMR (DMSO-*d*₆) 145.03, 143.50, 142.85, 140.77, 137.45, 127.33, 124.61, 122.18, 115.84, 110.61, 101.62 (figure S2 in Supplementary information). MS (ESI-MS): *m/z* calculated for C₁₁H₈N₆O₃, 272.07, found: [M-1]⁺, 270.9. (figure S3 in Supplementary information).

2.3 Preparation of solutions

The stock solutions of each anion (5 mM) of S²⁻, HSO₃⁻, S₂O₃²⁻, NO₂⁻, F⁻, Cl⁻, Br⁻, I⁻, CO₃²⁻, SO₄²⁻, OH⁻,

OAc⁻, SO₃²⁻, HCO₃⁻, HSO₄⁻, H₂PO₄⁻, HPO₄²⁻, PO₄³⁻, CN⁻ were prepared in deionized water from their sodium or potassium salts. Stock solution of **1** (1 mM) was prepared in acetonitrile. PBS buffer solutions (10 mM) were prepared by using proper amount of NaH₂PO₄ and Na₂HPO₄ under adjustment by a pH S-3C meter.

In titration experiments, **1** was diluted to a certain concentration (30 μM for absorption spectra and 10 μM for fluorescence spectra) with CH₃CN-PBS (10 mM, pH=7.2, 3:1, v/v). Then 3 mL of **1** CH₃CN-PBS (10 mM, pH=7.2, 3:1, v/v) was put into a quartz optical cell with an optical path of 1 cm. The stock solution of each anion was added into the quartz optical cell step by step via a microsyringe and the solution was stirred for 3 min before recording the spectra. For fluorescence measurements, excitation wavelength was set at 470 nm and emission was collected from 490 nm to 700 nm. The bandwidth of excitation and emission slits were both set at 5 nm. The quantum yields were measured using quinine sulfate in 1 N H₂SO₄ (*φ* = 0.54) as reference with excitation at 350 nm³⁹ using the following equation:

$$\phi_S = \phi_R \frac{A_R F_S n_S^2}{A_S F_R n_R^2} \quad (1)$$

where A and F are the absorbance and integrated fluorescence intensity, respectively, *n* is the refractive index of the solvent, and S and R represent the sample and reference, respectively.

3. Results and Discussion

3.1 Absorption properties

The absorption responses of probe **1** to various anions including S²⁻, HSO₃⁻, S₂O₃²⁻, NO₂⁻, F⁻, Cl⁻, Br⁻, I⁻, CO₃²⁻, SO₄²⁻, OH⁻, OAc⁻, SO₃²⁻, HCO₃⁻, HSO₄⁻, H₂PO₄⁻, HPO₄²⁻, PO₄³⁻, CN⁻ in CH₃CN-PBS (10 mM, pH=7.2, 3:1, v/v) were explored. Compound **1** alone showed a maximum absorption peak at 496 nm in

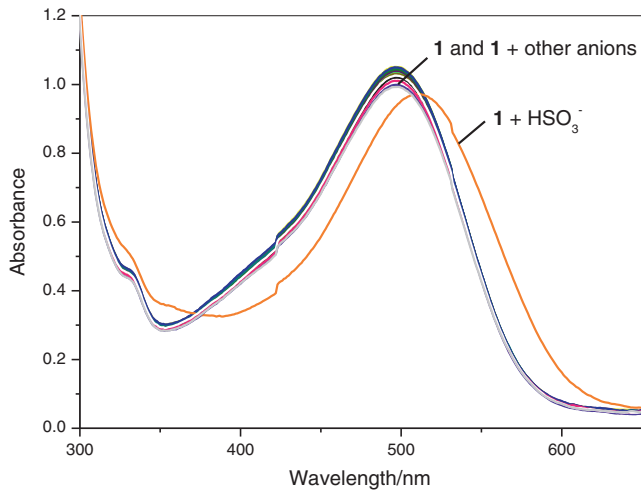


Figure 1. Absorption spectra of probe **1** ($30\ \mu\text{M}$) in the presence of various anions ($300\ \mu\text{M}$).

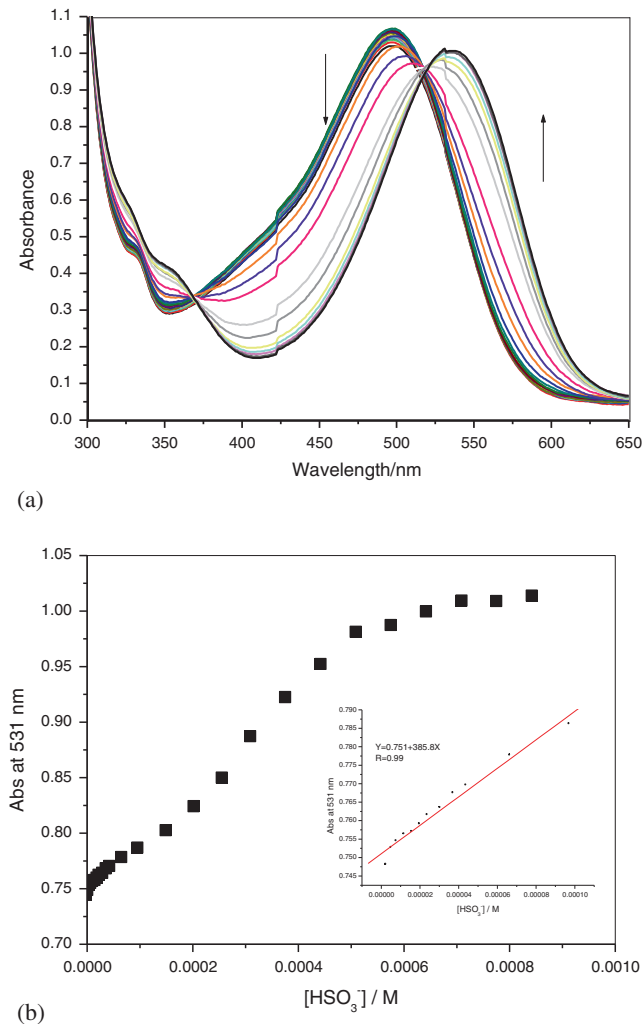


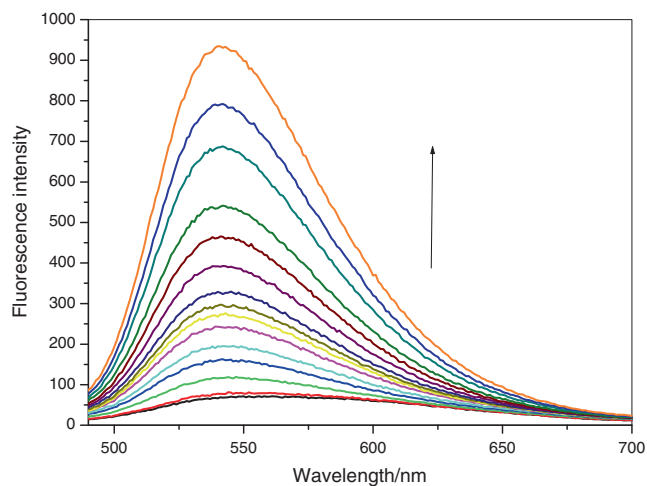
Figure 2. (a) Absorption spectra of **1** ($30\ \mu\text{M}$) in the presence of increasing concentrations of NaHSO_3 in CH_3CN - PBS ($10\ \text{mM}$, $\text{pH}=7.2$, $3:1$, v/v). (b) Absorbance at $531\ \text{nm}$ of **1** upon gradual addition of HSO_3^- , inset: Absorbance at $531\ \text{nm}$ of **1** vs HSO_3^- in the concentration range of $0 \sim 120\ \mu\text{M}$.

CH_3CN - PBS ($10\ \text{mM}$, $\text{pH}=7.2$, $3:1$, v/v). The peak at $496\ \text{nm}$ could be assigned as its internal charge transfer (ICT) absorption transition. The absorption spectrum of probe **1** was bathochromically shifted in the presence of HSO_3^- . However, the absorption profiles of probe **1** remained unchanged upon addition of other anions (figure 1). Upon addition of HSO_3^- , the absorbance at $496\ \text{nm}$ decreased gradually and was red-shifted until a new absorption peak at $531\ \text{nm}$ appeared and increased, indicating structural change upon interaction with bisulfite. Two isosbestic points at $368\ \text{nm}$ and $516\ \text{nm}$ appeared in the UV-vis spectra (figure 2a). The red solution of **1** in CH_3CN - PBS ($10\ \text{mM}$, $\text{pH}=7.2$, $3:1$, v/v) turned to a purple-red color upon addition of HSO_3^- . The absorbance at $531\ \text{nm}$ increased linearly with the increasing of the HSO_3^- concentration in the range of $2.7\ \mu\text{M} \sim 120\ \mu\text{M}$ (inset in figure 2b). Then, the absorbance increased only slightly with the increase of the concentration of HSO_3^- (figure 2b). The relationship between the absorbance at $531\ \text{nm}$ and HSO_3^- concentration in the linear regime is: $A = 385.8C + 0.751$, with a correlation coefficient of $R = 0.99$, where C is the concentration of HSO_3^- in mol/L . The detection limit, based on the definition by IUPAC was found to be $0.74\ \mu\text{M}$ from 11 blank solutions.

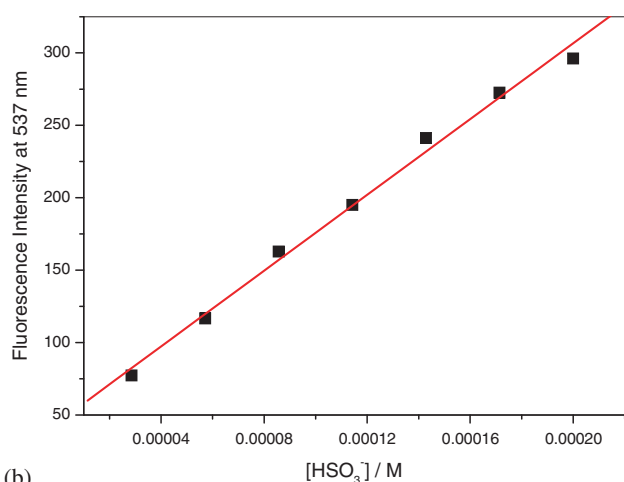
3.2 Fluorescence properties

The fluorescence responses of **1** with different concentrations of HSO_3^- in CH_3CN - PBS ($10\ \text{mM}$, $\text{pH}=7.2$, $3:1$, v/v) were measured (figure 3a). When excited at $470\ \text{nm}$, **1** showed a very weak fluorescence band centered at $540\ \text{nm}$ ($\phi < 0.001$). The titration of HSO_3^- to **1** demonstrated an obvious emission increase of the band with slight blue-shift to $537\ \text{nm}$. When $450\ \mu\text{M}$ bisulfite was added, nearly 10-fold fluorescent enhancement was obtained ($\phi = 0.237$). The fluorescence intensity increased linearly with increasing of the HSO_3^- concentration in the range of $0 \sim 300\ \mu\text{M}$ (figure 3b). The relationship between the fluorescence intensity at $537\ \text{nm}$ and HSO_3^- concentration was: $I = 1.31 \times 10^6 C + 44.94$, with a correlation coefficient of $R = 0.9965$, where C is the concentration of HSO_3^- in M . The detection limit, based on the definition by IUPAC was found to be $50.6\ \text{nM}$ from 11 blank solutions. The fluorescent results indicated that compound **1** is suitable for use as a fluorescent probe for bisulfite.

Job's plot analysis⁴⁰ using fluorescence method with a total concentration of $40\ \mu\text{M}$ at $537\ \text{nm}$ revealed a maximum at about 0.5 mole fraction (figure 4), indicating 1:1 binding stoichiometry of **1** and HSO_3^- . The association constant⁴¹ was calculated to be $1016\ \text{M}^{-1}$ by using a Benesi-Hildebrand plot according to the



(a)



(b)

Figure 3. (a) Fluorescence spectra of of **1** (10 μM) in the presence of increasing concentrations of HSO_3^- (0~57 μM) in $\text{CH}_3\text{CN-PBS}$ (10 mM, pH=7.2, 3:1, v/v). Excitation wavelength is 470 nm. Bandwidth of both ex slit and em slit were set at 5 nm. (b) Fluorescence intensity at 537 nm of **1** vs concentration of HSO_3^- in the range of 29 μM ~300 μM .

fluorescence titration profile (figure S4, Supplementary material).

After adding 400 μM of anions, such as S^{2-} , HSO_3^- , $\text{S}_2\text{O}_3^{2-}$, NO_2^- , F^- , Cl^- , Br^- , I^- , CO_3^{2-} , SO_4^{2-} , OH^- , OAc^- , SO_3^{2-} , HCO_3^- , HSO_4^- , H_2PO_4^- , HPO_4^{2-} , PO_4^{3-} , CN^- respectively to the $\text{CH}_3\text{CN-PBS}$ (10 mM, pH=7.2, 3:1, v/v) solution containing 10 μM of **1** for 3 min, only HSO_3^- induced a significant fluorescence enhancement at 537 nm (figure 5). Other anions including S^{2-} , $\text{S}_2\text{O}_3^{2-}$, NO_2^- , F^- , Cl^- , Br^- , I^- , CO_3^{2-} , SO_4^{2-} , OH^- , OAc^- , SO_3^{2-} , HCO_3^- , HSO_4^- , H_2PO_4^- , HPO_4^{2-} , PO_4^{3-} , CN^- showed little changes in fluorescence spectra under the same conditions. The competition experiments indicated that less obvious fluorescent changes of probe **1** were observed in the presence of 40 equiv. of other anions. Upon further addition of 40 equiv. of

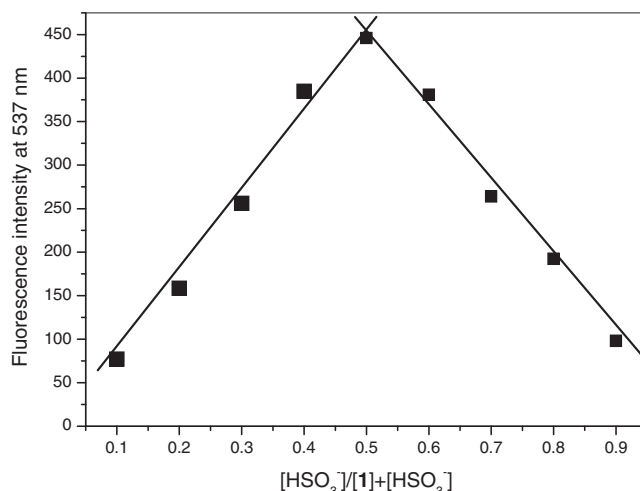


Figure 4. Job's plot for determining the stoichiometry of **1** and HSO_3^- in $\text{CH}_3\text{CN-PBS}$ (10 mM, pH=7.2, 3:1, v/v) with a total concentration of 40 μM . Excitation wavelength is 470 nm. Band width of ex slit and em slit were set at 5 and 10 nm, respectively.

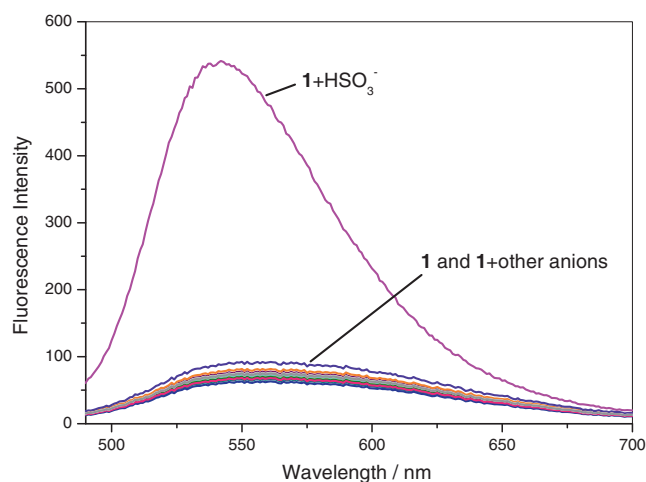


Figure 5. Fluorescence spectra of probe **1** (10 μM) in the presence of various anions (400 μM).

HSO_3^- to the solution which containing probe **1** and 40 equiv. of competing anions, the change of the emission was similar to that as observed in the **1**- HSO_3^- solution (figure 6). As a result, probe **1** displayed high selectivity to detect HSO_3^- even in the presence of 40 equiv of other anions.

3.3 Molecular calculations

To understand the recognition process of **1** toward HSO_3^- , HOMO and LUMO distributions of **1** and **1**- HSO_3^- (assuming that HSO_3^- was bound to **1**) were determined by density functional theory (DFT) calculations at the B3LYP/6-31G* level using Gaussian 03

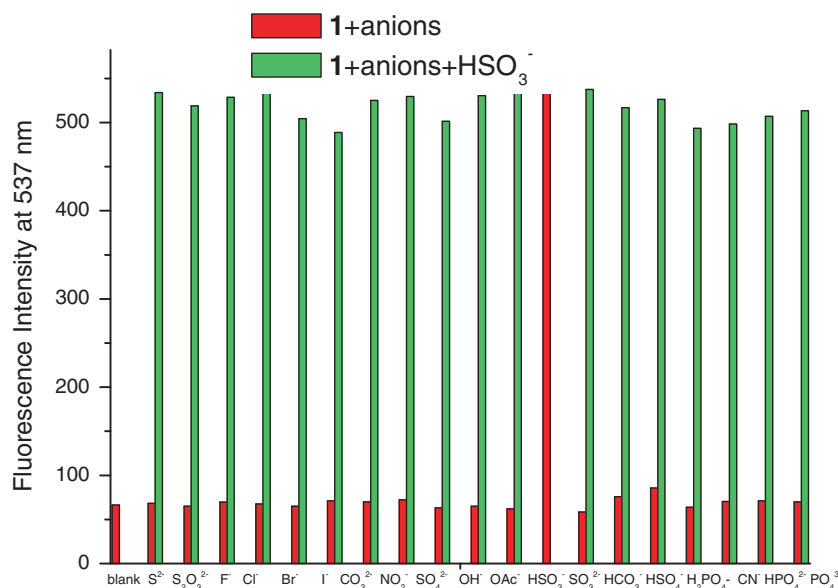


Figure 6. Selectivity of **1** ($10 \mu\text{M}$) for HSO_3^- in the presence of other anions ($400 \mu\text{M}$) in $\text{CH}_3\text{CN-PBS}$ (10 mM , $\text{pH}=7.2$, $3:1$, v/v), red bars represent: blank, S^{2-} , $\text{S}_2\text{O}_3^{2-}$, F^- , Cl^- , Br^- , I^- , CO_3^{2-} , NO_2^- , SO_4^{2-} , OH^- , OAc^- , HSO_3^- , SO_3^{2-} , HCO_3^- , HSO_4^- , H_2PO_4^- , HPO_4^{2-} , PO_4^{3-} , CN^- . Green bars represent the results for subsequent addition of HSO_3^- ($400 \mu\text{M}$) to the solution. Excitation wavelength is 470 nm . Bandwidth of both ex slit and em slit were set at 5 nm .

program.⁴² As shown in figure 7, the NBD moiety, schiff base and pyrrole group of **1** were in the planar structure. The HOMO distribution of **1** was mainly

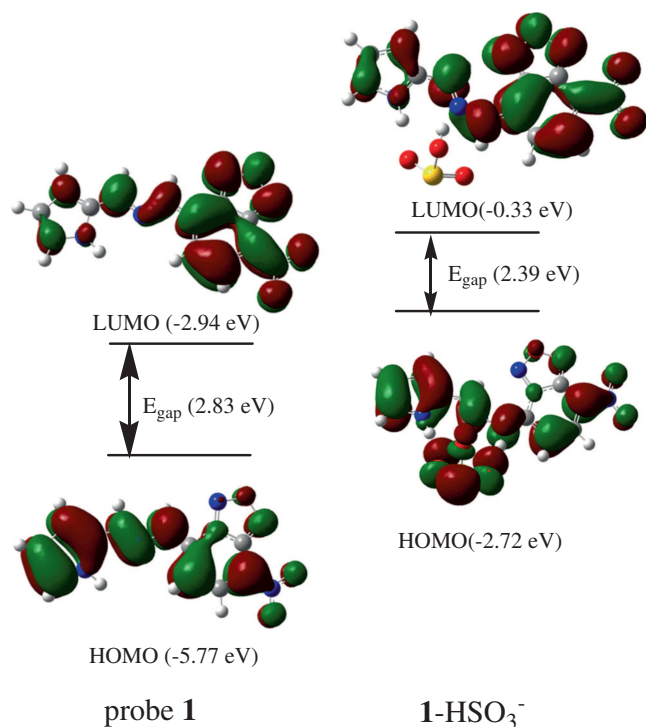
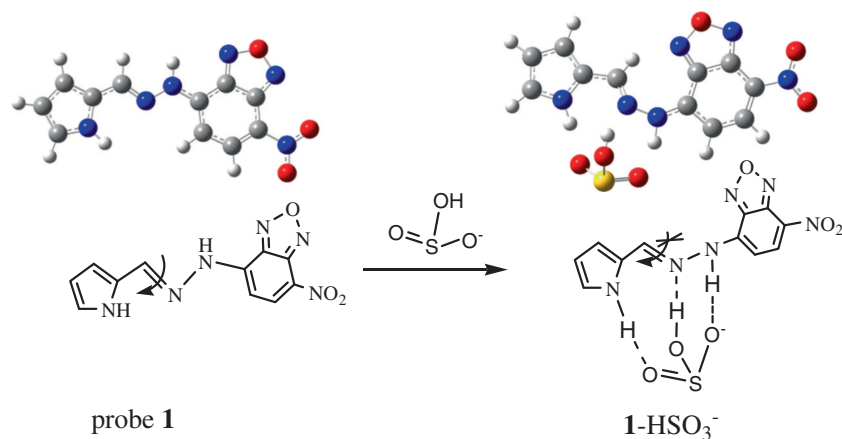


Figure 7. Calculated HOMO and LUMO distribution of probe **1** and its complex 1-HSO_3^- .

concentrated on the pyrrole group. The electron donor property of the pyrrole group was responsible for fluorescence quenching through PET effect (photoinduced electron transfer). Furthermore, the $\text{C}=\text{N}$ isomerization would also contribute to the nonfluorescent property of **1**. It could be found that the NBD hydrazine moiety and the pyrrole group were *trans* to each other across the $\text{C}=\text{N}$ to keep its stable structure, after the formation of 1-HSO_3^- . Before the formation of 1-HSO_3^- , the N-N σ bond in hydrazine could be free to rotate. After the addition of bisulfite, probe **1** had three sites for hydrogen bonding with the anion, one NH moiety on the NBD hydrazine, one NH on pyrrole and one N atom in the schiff base to interact with the H atom of hydroxyl in HSO_3^- (scheme 2). The calculated hydrogen bonding distances were 1.6204 \AA , 1.7634 \AA and 2.1757 \AA respectively. These hydrogen bonding interaction can restrict the free rotation of the N-N σ bond in hydrazine and increase the structural rigidity of **1**. The interaction with bisulfite caused a non-coplanar structure of probe **1** (The dihedral angle was changed from 0° to 1.2787° after its interaction with HSO_3^-), which blocked the PET process and induced the enhancement of its fluorescence. Moreover, the energy gap between the HOMO and LUMO of 1-HSO_3^- was smaller than that of probe **1**, in good agreement with the red shift of absorption spectra of probe **1** upon reaction with HSO_3^- . The hydrogen bond-inhibited $\text{C}=\text{N}$ isomerization-reduced



Scheme 2. Possible structure of 1:1 binding of probe **1** with bisulfite.

quenching mechanism⁴³ could also be used to explain the interaction between probe **1** and HSO_3^- . In this case, the NBD hydrazine moiety and the pyrrole group had to keep *trans* to each other across the $\text{C}=\text{N}$ for the formation of three hydrogen bonds with HSO_3^- .

3.4 MS analysis

The data of ESI mass spectrum provided further evidence of the formation of a 1:1 $\mathbf{1}\text{-HSO}_3^-$ complex in

$\text{CH}_3\text{CN}/\text{H}_2\text{O}$ (3:1, v/v) solution (figure S5 in Supplementary information). The peak at $m/z=358.97$ (calcd. 359.02), corresponding to $[\mathbf{1}+\text{HSO}_3\text{-OH}+\text{Na}]^+$, was observed when HSO_3^- (4 mM) is added to **1** (0.1 mM), whereas free **1** exhibited a peak at $m/z=270.9$, which corresponds to $[\mathbf{1}\text{-H}]^+$ (figure S3 in Supplementary information). The MS data was considered to support the proposed recognition mechanism, indicating the two NH groups and N atom in $\text{C}=\text{N}$ as anion binding sites.

Table 1. Determination results for bisulfite in real samples^a.

Sample	Added (μM)	Found (μM)	Recovery (%)	RSD (%)
White wine	0	6.2	–	3.1
	10	16.8	103.7	3.0
	50	55.9	99.3	2.8
	100	105.0	98.9	2.9
Red wine	0	13.7	–	2.8
	10	23.2	97.9	2.5
	50	63.1	99.1	2.7
	100	116.2	102.2	2.4
Beer	0	7.1	–	2.7
	10	17.7	103.5	3.1
	50	56.1	98.2	3.0
	100	109.0	101.8	2.8

^a Bisulfite concentrations were determined using a standard addition method^{43–45} by measuring increase of the fluorescence intensity of **1** at 537 nm. The standard curve in figure S6 was used to extrapolate the unknown amount of bisulfite. Aliquots of the sample solution which was diluted 10-fold were added to CH_3CN -PBS (10 mM, pH=7.2, 3:1, v/v) containing probe **1** (5 μM), and the emission intensity at 537 nm was recorded, whereby the unknown concentrations of bisulfite were determined. For recovery studies, known concentrations of bisulfite were added to each sample and the total bisulfite concentration was determined following the method described above. Relative standard deviations were calculated on the basis of five measurements.

3.5 Real sample analysis

Probe **1** was used to examine the content of bisulfite in real life samples. White wine, red wine and beer bought from a supermarket were diluted 10-fold with deionized water and analyzed by standard addition and recovery experiments. As shown in table 1, probe **1** was found to be suitable to determine the concentration of bisulfite with good recoveries in these samples. The bisulfite content in white wine, red wine and beer were 6.2, 13.7 and 7.1 μM , respectively.

4. Conclusion

A simple novel fluorescent probe based on NBD chromophore (probe **1**) for turn-on and selective detection of bisulfite was developed. The absorption spectrum of probe **1** was bathochromically shifted and the fluorescence of **1** was greatly enhanced in the presence of HSO_3^- . From the MS analysis and DFT calculations, two NH moieties and one N atom in $\text{C}=\text{N}$ of probe **1** were considered to interact with bisulfite through three hydrogen bondings. These hydrogen-bonding interactions would restrict the free rotation of the N-N σ bond in hydrazine and increase the structural rigidity of **1**,

block the PET process and inhibit C=N isomerization, resulting in significant fluorescent enhancement of **1**.

Supplementary Information

All additional information about ^1H NMR (figure S1), ^{13}C NMR (figure S2), MS spectrum (figure S3) of compound **1**, Benesi-Hildebrand plot (figure S4), MS spectrum of **1** HSO_3^- (figure S5) and the standard curve in figure S6 are given in the supplementary information. Supplementary information is available at www.ias.ac.in/chemsci.

Acknowledgement

This project was supported by the National Natural Science Foundation of China (NSFC, No.21102037).

References

- Rostami A and Taylor M S 2012 *Macromol. Rapid Commun.* **33** 21
- Kim S K, Kim H N, Zhu X, Lee H N, Soh J H, Swamy K M K and Yoon J 2007 *Supramol. Chem.* **19** 221
- Kobayashi H, Ogawa M, Alford R, Choyke P L and Urano Y 2010 *Chem. Rev.* **110** 2620
- Gale P A, Garcia-Garrido S E and Garric J 2008 *Chem. Soc. Rev.* **37** 151
- Suksai C and Tuntulani T 2003 *Chem. Soc. Rev.* **32** 192
- O'Neil E J and Smith B D 2006 *Coord. Chem. Rev.* **250** 3068
- Davis A P 2006 *Coord. Chem. Rev.* **250** 2939
- Sessler J L, Camiolo S and Gale P A 2003 *Coord. Chem. Rev.* **240** 17
- Bondy C R and Loeb S J 2003 *Coord. Chem. Rev.* **240** 77
- Choi K and Hamilton A D 2003 *Coord. Chem. Rev.* **240** 101
- Gale P A 2006 *Acc. Chem. Res.* **39** 465
- Schmuck C 2006 *Coord. Chem. Rev.* **250** 3053
- Schug K A and Lindner W 2005 *Chem. Rev.* **105** 67
- Yoon J, Kim S K, Singh N J and Kim K S 2006 *Chem. Soc. Rev.* **35** 355
- Best M D, Tobey S L and Anslyn E V 2003 *Coord. Chem. Rev.* **240** 3
- Xu Z, Kim S K and Yoon J 2010 *Chem. Soc. Rev.* **39** 1457
- Llinares J M, Powell D and Bowman-James K 2003 *Coord. Chem. Rev.* **240** 57
- Beer P D and Hayes E J 2003 *Coord. Chem. Rev.* **240** 167
- Steed J W 2009 *Chem. Soc. Rev.* **38** 506
- Rice C R 2006 *Coord. Chem. Rev.* **250** 3190
- Amendola V and Fabbrizzi L 2009 *Chem. Commun.* **5** 513
- Jun M E, Roy B and Ahn K H 2011 *Chem. Commun.* **47** 7583
- Peng X J, Wu Y K, Fan J L, Tian M Z and Han K L 2005 *J. Org. Chem.* **70** 10524
- McFeeters R F 1998 *J. Food Prot.* **61** 885
- Yang X, Guo X and Zhao Y 2002 *Anal. Chim. Acta* **456** 121
- Fazio T and Warner C R 1990 *Food Addit. Contam.* **7** 433
- Decnop-Weever L G and Kraak J C 1997 *Anal. Chim. Acta* **337** 125
- Verma S K and Deb M K 2007 *J. Agric. Food Chem.* **55** 8319
- Huang Y M, Zhang C, Zhang X R and Zhang Z J 1999 *Anal. Chim. Acta* **391** 95
- Bush R K, Taylor S L and Busse W J 1986 *J. Allergy Clin. Immunol.* **78** 191
- Yang Y T, Huo F J, Zhang J J, Xie Z H, Chao J B, Yin C X, Tong H B, Liu D S, Jin S, Cheng F Q and Yan X X 2012 *Sens. Actuators B* **166** 665
- Taylor S L, Hagle N A and Bush R K 1986 *Adv. Food Res.* **30** 1
- Nichol G M, Parsons G H and Chung K F 1994 *Br. J. Pharmacol.* **111** 918
- Reist M, Jenner P and Halliwell B 1998 *FEBS Lett.* **423** 231
- Lavis L D and Raines R T 2008 *ACS Chem. Biol.* **3** 142
- Lakowicz J R 2006 In *Principles of fluorescence spectroscopy*. 3rd ed. (New York: Springer) p.15
- Loura L M S, Fernandes F, Fernandes A C and Ramalho J P P 2008 *BBA- Biomembranes* **1778** 491
- Key J A, Li C and Cairo C W 2012 *Bioconjug. Chem.* **23** 363
- Birks J B 1970 In *Photophysics of Aromatic Molecules* (New York: Wiley-Interscience)
- Connors K A 1987 In *Binding Constants-The Measurement of Molecular Complex Stability* (New York: John Wiley & Sons)
- Benesi H and Hildebrand J 1949 *J. Am. Chem. Soc.* **71** 2703
- Frisch M J, Trucks G W, Schlegel H B, Scuseria G E, Robb M A, Cheeseman J R, Montgomery J A, Vreven Jr T, Kudin K N, Burant J C, Millam J M, Iyengar S S, Tomasi J, Barone V, Mennucci B, Cossi M, Scalmani G, Rega N, Petersson G A, Nakatsuji H, Hada M, Ehara M, Toyota K, Fukuda R, Hasegawa J, Ishida M, Nakajima T, Honda Y, Kitao O, Nakai H, Klene M, Li X, Knox J E, Hratchian H P, Cross J B, Bakken V, Adamo C, Jaramillo J, Gomperts R, Stratmann R E, Yazyev O, Austin A J, Cammi R, Pomelli C, Ochterski W J, Ayala P Y, Morokuma K, Voth G A, Salvador P, Dannenberg J J, Zakrzewski V G, Dapprich S, Daniels A D, Strain M C, Farkas O, Malick D K, Rabuck A D, Raghavachari K, Foresman J B, Ortiz J V, Cui Q, Baboul A G, Clifford S, Cioslowski J, Stefanov B B, Liu G, Liashenko A, Piskorz P, Komaromi I, Martin R L, Fox D J, Keith T, Al-Laham M A, Peng C Y, Nanayakkara A, Challacombe M, Gill P M W, Johnson B, Chen W, Wong M W, Gonzalez C and Pople J A 2003 *Gaussian 03*, revision B05, Wallingford, CT
- Sun Y -Q, Wang P, Liu J, Zhang J and Guo W 2012 *Analyst* **137** 3430
- Ros-lis J V, García B, Jiménez D, Martínez-Máñez R, Sancenón F, Soto J, Gonzalvo F and Valdecabres M C 2004 *J. Am. Chem. Soc.* **126** 4064
- Liao W, Wu F, Wu Y and Wang X 2008 *Microchim. Acta.* **162** 147